

Acidic and basic properties of nitramide, and the catalysed decomposition of nitramide and related compounds: an *ab initio* theoretical investigation †

2 PERKIN

Mirjana Eckert-Maksić,^{*a} Howard Maskill^{*b} and Irena Zrinski^a

^a Department of Chemistry and Biochemistry, Ruđer Bošković Institute, POB 180, HR-10002 Zagreb, Croatia. E-mail: mmaksic@emma.irb.hr

^b Chemistry Department, University of Newcastle, Newcastle upon Tyne, UK NE1 7RU. E-mail: h.maskill@ncl.ac.uk

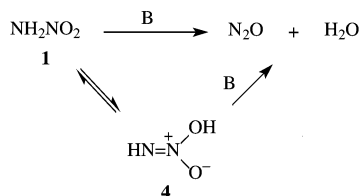
Received (in Cambridge, UK) 8th June 2001, Accepted 17th August 2001

First published as an Advance Article on the web 9th October 2001

Deprotonation from nitrogen of the *aci*-nitro tautomer (**4**) of nitramide (**1**) has been shown to give an anion which does not correspond to an energy minimum on the potential energy surface. The base-catalysed decomposition of nitramide *via* this tautomer, therefore, occurs by an enforced concerted mechanism which, on the basis of previously reported experimental results, is deduced to be highly asynchronous. Protonation of **4** on the hydroxy also leads to an ion which spontaneously fragments, consequently the acid-catalysed decomposition of **1** *via* **4** also involves concerted proton transfer and fragmentation. The uncatalysed decomposition of nitramide through the same tautomer **4** is also concerted, and the mechanism through a cyclic transition structure involving two water molecules is shown to be more favourable than a cyclic concerted mechanism involving a single water molecule. Structures and energies of all relevant species have been calculated and shown to be in good agreement with experimental results where these are available.

Introduction

The base-catalysed decomposition of nitramide (**1**), Scheme 1, is

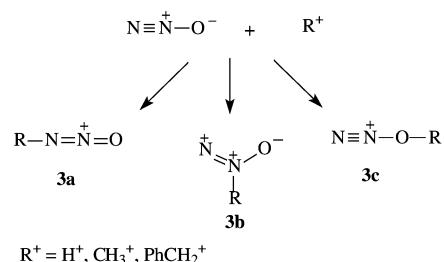


Scheme 1 The base-catalysed decomposition of nitramide.

one of the defining reactions of what became physical organic chemistry even though **1** is not an organic compound. It was one of the principal reactions used to test theories and mechanisms of catalysis in homogeneous solution, and was investigated quantitatively in pioneering work from the early years of the twentieth century.¹ The reaction was shown to be catalysed by a wide range of bases from which it was deduced that the rate-limiting step involves proton abstraction, and the focus was generally upon how the nature of the base affects this step. Many experimental results relating to this matter have been reported and their interpretation led to significant advances in our understanding of acid–base catalysis and, in particular, the discovery of the Brønsted relationship.^{1,2} The acid-catalysed decomposition of **1**, although also detected long ago, has attracted much less attention and is significant only in strongly acidic media;³ nitramines, RNHNO₂, the *N*-alkyl analogues of nitramide, undergo the same type of reaction as the parent under acidic conditions, but not under basic conditions.

† Electronic supplementary information (ESI) available: selected geometrical parameters, energies and zero point energies of nitramide **1**, its *aci*-nitro isomers **4a–d**, anion **7**, and molecular complexes **MCI** and **MCI'** calculated at MP2/6-31G** and MP2/6-311++G** levels of theory. See <http://www.rsc.org/suppdata/p2/b1/b105074p/>

Following our earlier experimental investigations into the solvolytic decomposition of *p*-tolylsulfonyloxy-*NNO*-azoxyalkanes (**2**)⁴ (Fig. 1), we collaborated in an *ab initio* theoretical study of potential intermediates, (RN₂O)⁺.⁵ By considering the energetics of adding electrophiles R⁺ = H⁺, CH₃⁺, and PhCH₂⁺ to each of the three atoms of a nitrous oxide molecule (Scheme 2), it was established that bonded species are obtained



Scheme 2 Addition of electrophiles to nitrous oxide.

only by adding the electrophiles to the terminal atoms. Those obtained by bonding to the oxygen (**3c**) were calculated to be more stable than the isomers with bonding to the terminal nitrogen (**3a**); structures corresponding to bonding with the central nitrogen (**3b**) did not correspond to energy minima. Thus, any chemical reaction which has the potential to generate an intermediate corresponding to **3b** will necessarily bypass the potential intermediate in an enforced concerted mechanism.⁶ In contrast, potential intermediates analogous to **3a** or **3c** are not excluded by these theoretical considerations, and whether either of them actually intervenes in a reaction will be determined by other factors.

The uncatalysed reactions of azoxyalkanes (**2**) relate to the acid-catalysed reaction of alkyl nitramines (see below), our consideration of which, in turn, led to a theoretical investigation of the acidic and basic properties of the parent nitramide and its decomposition catalysed by acids and bases. We adopted

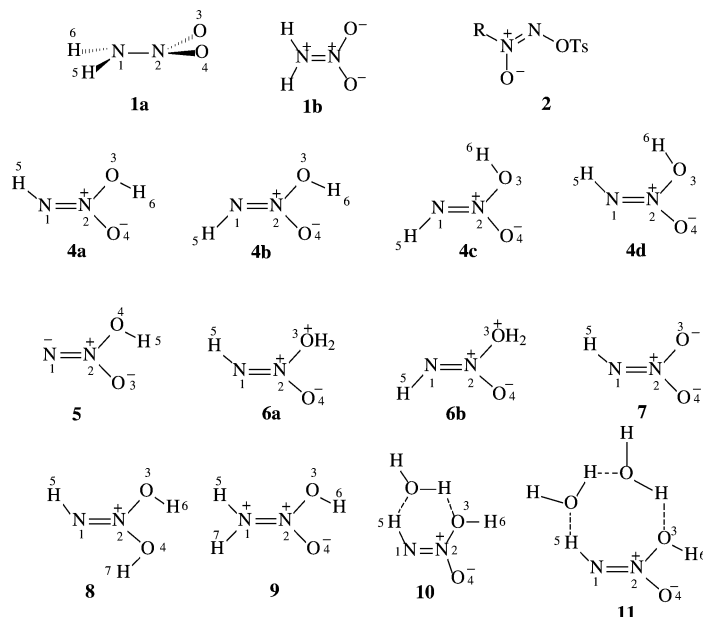


Fig. 1

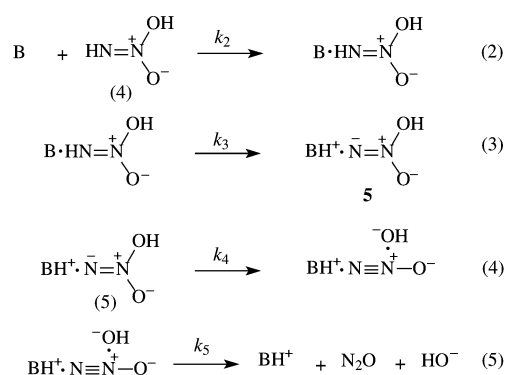
the same strategy of investigating possible intermediates computationally, and now report results which, *inter alia*, allow refinement of our mechanistic understanding of the acid- and base-catalysed decompositions of nitramide and the acid-catalysed decomposition of *N*-alkylnitramines. Intermediates previously invoked in these reactions must be rejected as they do not correspond to stable bonded species.

The structure and acid–base properties of nitramide

Nitramide is not easy to prepare and purify, and has a tendency to explode at elevated temperatures. Nevertheless, its structure has been determined by X-ray crystallography and spectroscopic methods.^{7,8} Application of current *ab initio* theoretical methods leads to a structure in good agreement with experiment.⁹ The molecule is appreciably pyramidal at the NH₂ and slightly pyramidal at the NO₂, structure **1a** in Fig. 1. The barrier to inversion at the NH₂ has been calculated to be 2.2 kcal mol⁻¹ in agreement with experiment (and compares with 5.8 and 4.8 kcal mol⁻¹ for ammonia and methylamine, respectively), and the barrier to internal rotation was calculated to be *ca.* 10–12 kcal mol⁻¹. There appears to be no evidence of appreciable delocalisation of the lone pair on the amino into the nitro group in the gas phase, **1b** in Fig. 1. Mass spectrometric experimental work by Cacace and co-workers supported by G2 calculations indicated that oxygen in nitramide is more basic than the amino nitrogen in the gas phase.¹⁰ Their studies also showed that nitramide is a relatively strong proton donor in the gas-phase—comparable with formic acid, for example.

Base-catalysed decomposition of nitramide

The evidence that the rate-determining step of the base-catalysed decomposition of nitramide to give nitrous oxide and water follows isomerisation of **1** to its *aci*-nitro form, **4** in Scheme 1, is convincing.^{1,11} The most recent comprehensive investigation of this reaction by Kresge and co-workers deployed various techniques, and involved a much improved experimental procedure for measuring rates of the reaction.¹¹ Their results using a range of oxygen and nitrogen bases with $-\log(qK_a/p) = 1-8$ led to an excellent linear Brønsted correlation with $\beta = 0.79$; deuterium kinetic isotope effect measurements over this range were consistently modest at $k_H/k_D = 2-3$. The proposed mechanism for the reaction of **4** is outlined in Scheme 3 where the stereochemistry of **4** is not specified; the

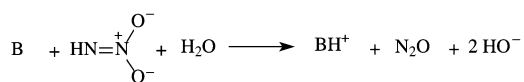


Scheme 3 Step-wise mechanism for the base catalysed decomposition of nitramide.

authors proposed that the rate-limiting step *follows* the proton transfer of eqn. (3). In other words, proton transfer and heavy atom rebonding are separate steps (rather than concerted), with the former being complete *before* the rate-limiting step (rather than part of it). On the grounds that diffusional separation of products, eqn. (5), is unlikely to be rate limiting, Kresge and co-workers proposed that eqn. (4) is the rate-limiting step under their reaction conditions, and provided convincing supportive arguments.

Downwards curvature in the Brønsted plot was observed with stronger bases and, with some such nitrogen bases, the deuterium kinetic isotope effect increased to $k_H/k_D \sim 5$. According to the mechanism in Scheme 3, these stronger bases would stabilise the product side of eqn. (3) leading to increased values for k_3 and lower values for k_{-3} (not shown in Scheme 3). Hence, at some stage, separation of the hydroxide as nucleofuge (k_4 , which will be largely unaffected by the increased strength of the base) becomes faster than the k_{-3} step; the k_3/k_{-3} barrier is now the highest, *i.e.* proton transfer is rate limiting. This step-wise mechanism requires that the anion **5** (Fig. 1) of the ion-pair product of eqn. (3) be a properly bonded intermediate with a finite lifetime.

With their considerably improved spectroscopic method for measuring rates of nitramide decomposition, Kresge and co-workers were also able to identify a second reaction pathway in more strongly basic aqueous solution.¹² The mechanism they proposed for this pathway involves rate-limiting proton transfer from deprotonated nitramide to the base as shown in

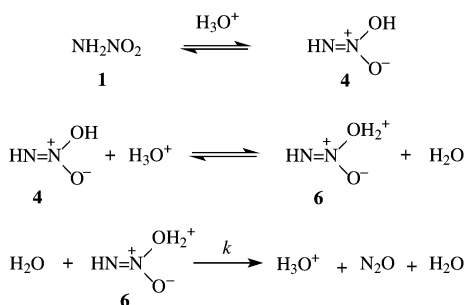


Scheme 4 Rate-limiting proton transfer from deprotonated nitramide under strongly basic conditions.

Scheme 4. To avoid formation of the highly unstable O^{2-} in aqueous solution, they proposed that this base-induced fragmentation of the anionic substrate is concerted with a second proton transfer from a water molecule to the incipient oxide anion.

Acid-catalysed decomposition of nitramide

Although the acid-catalysed decomposition of nitramide was reported many years ago,³ it is only recently that the reaction has been investigated by modern techniques. Cox has used the excess acidity method in aqueous perchloric, hydrochloric, and sulfuric acids to characterise not only the acid-catalysed pathway, but also the water-induced reaction.¹³ In both, the initial step is isomerisation of **1** to the *aci*-nitro form (**4**), as under basic conditions. The mechanism proposed by Cox for acid catalysis is outlined in Scheme 5 and involves equilibrium

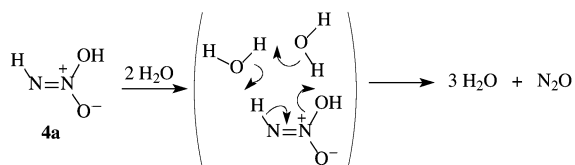


Scheme 5 Step-wise mechanism for the acid-catalysed decomposition of nitramide.

protonation of the hydroxy of the *aci*-nitro form to give (*E*)- or (*Z*)-**6**. Either or both of these diastereoisomeric intermediates may then undergo rate-limiting abstraction of a proton from nitrogen by water concerted with departure of the protonated hydroxy nucleofuge as a water molecule from the other nitrogen. In sulfuric acid, the sulfate anion may also act as a base in a parallel pathway which accounts for its modest rate-enhancing effect. In both routes, **6** is proposed as an intermediate of finite lifetime formed by reversible protonation of **4**.

Uncatalysed decomposition of nitramide

In the very slow water-induced reaction, also *via* **4**, Cox proposed that hydrogen bonding by a water molecule assists departure of hydroxide as nucleofuge from one end in concert with another water molecule acting as a base at the other end, these two water molecules themselves being connected by a hydrogen bond in the cyclic mechanism indicated in Scheme 6.



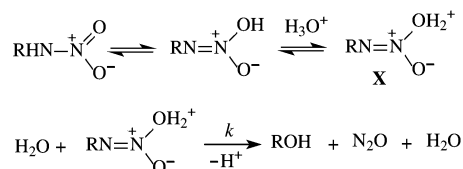
Scheme 6 Concerted cyclic mechanism for the uncatalysed decomposition of nitramide.

Whilst lacking definitive evidence, this mechanism for the uncatalysed reaction is wholly credible, well precedented, and requires reaction from the *Z*-diastereoisomer of **4** (**4a** in Fig. 1)

rather than the *E*, as shown in Scheme 6. However, it is qualitatively different from the acid- and base-catalysed mechanisms (see above) as it is a fully concerted process without the involvement of an intermediate.

Acid-catalysed decomposition of *N*-alkylnitramines

Cox proposed a mechanism similar to that in Scheme 5 for the acid-catalysed reaction of alkylnitramines (which have no appreciable reactivity in non-acidic solution) but with the water molecule acting as a nucleophile (to give the alkanol product) rather than as a base¹⁴ (Scheme 7). In this step-wise mechanism,



Scheme 7 Step-wise mechanism for the acid-catalysed decomposition of *N*-alkylnitramines.

intermediates are invoked which, like those in the mechanism of Scheme 5, can also exist as *E* and *Z* forms. The rate-limiting step of this mechanism represents a bimolecular solvent-induced analogue of the unimolecular mechanism proposed some years ago for the uncatalysed solvolytic decomposition of azoxyalkanes, **2**.⁴ In that reaction, no bimolecular fragmentation arising from nucleophilic attack at R was detected; if alkyl azoxyoxysulfonylarenes do suffer direct bimolecular attack by nucleophiles more potent than water or alcohols, it is at sulfur with a quite different electron flow.¹⁵ The mechanism in Scheme 7 involves the reversibly formed *E* or *Z* protonated *aci*-nitro form of the substrate, **X** (analogous to **6** in Scheme 5), as an intermediate with a finite lifetime.

Computational methods

All calculations reported here were performed with the Gaussian 94 and Gamess-US suite of programs on Unix-based Pentium III PCs.^{16,17} Geometry optimisation of **1**, its isomers (**4a-d**), their deprotonated forms (**5** and **7**), and protonated forms (**6a-b**, **8**, and **9**) were carried out at different levels of theory including MP2/6-31G**, MP2/6-31+G**, and MP2/6-311++G**. Only the results of MP2/6-31+G** will be discussed here, unless otherwise noted. This basis set includes polarisation functions at the hydrogen atoms and diffuse functions which are well known to be necessary for the reliable description of hydrogen bonds and energies of anionic species, respectively.¹⁸ Results of other calculations are listed in Table 1s† of the supporting material for comparison. After geometry optimisations, vibrational frequencies were calculated at the same level of theory to determine the nature of stationary points and to calculate zero level vibrational energies. Additional calculations were carried out on complexes of some *aci*-nitro isomers of **1** with water, their protonated forms, and at points on the potential energy surface (PES) for their decomposition in the gas phase and in water. From among a variety of structures which were considered, only the most important ones for understanding the mechanism of nitramide decomposition will be discussed below. Gas phase calculations were done at the MP2/6-31+G** level of theory and were corrected for the basis set superposition error (BSSE),¹⁹ while energies in water were computed by modeling the solvent with the isodensity polarizable continuum method²⁰ (IPCM) with relative permittivity $\epsilon = 78.5$ but otherwise at the same level (MP2/6-31+G**). Hydration energies were calculated without zero point energy (ZPE), since the IPCM method is only available for single-point calculations and hence no vibrational analysis can be carried out. Connection of the transition structure between designated

Table 1 Selected structural parameters of nitramide **1**, its *aci*-nitro isomers **4a–d**, anion **7**, and cations **8** and **9** optimized at the MP2/6-31+G** level of theory

Geometric parameters	1	4a	4b	4c	4d^a	7	8	9
Bond/Å								
N(1)–N(2)	1.397(1.381) ^b	1.273	1.278	1.285	1.280	1.321(1.320) ^c	1.236	1.301(1.300) ^c
N(1)–H(5)	1.013(1.007) ^b	1.022	1.025	1.024	1.021	1.023	1.030	1.016(1.201) ^c
N(2)–O(3)	1.237(1.232) ^b	1.447	1.399	1.401	1.470	1.273(1.284) ^c	1.330	1.348(1.346) ^c
N(2)–O(4)	1.237(1.232) ^b	1.224	1.240	1.227	1.212	1.292(1.270) ^c	1.332	1.209(1.207) ^c
O(3)–H(6)	—	0.976	0.975	0.977	0.972	—	0.985	0.985(0.993) ^c
O(3)–H(5)	—	2.182	—	—	2.284	—	2.345	2.294
O(4)–H(6)	—	2.180	2.147	—	2.887	—	2.148	2.279
O(4)–H(5)	—	—	2.349	2.369	—	—	—	—
N(1)–H(6)	—	—	—	2.136	—	—	—	—
Angle/degree								
H(5)–N(1)–N(2)	109.0	105.4	103.3	104.4	106.2	101.7(100.9) ^c	109.0	118.3(118.4) ^c
N(1)–N(2)–O(4)	116.3	129.2	132.3	132.4	128.4	119.1(118.7) ^c	122.8	125.7(125.7) ^c
O(4)–N(2)–O(3)	127.4(132.7) ^b	115.7	116.2	114.4	113.3	119.9(120.2) ^c	111.8	123.3(123.4) ^c
N(2)–O(3)–H(6)	—	101.8	101.6	102.8	103.4	—	107.9	105.6(105.4) ^c
H(5)–N(1)–H(6)	115.1(120.9) ^b	—	—	—	—	—	—	—
H(6)–N(1)–N(2)–O(3)	28.7	—	—	—	—	—	—	—
H(6)–N(1)–N(2)–H(5)	126.4	—	—	—	—	—	—	—
O(3)–N(2)–N(1)–O(4)	176.3	—	—	—	—	—	180.0	180.0(180.0) ^c
H(5)–N(1)–N(2)–O(4)	—	180.0	0.0	0.0	173.0	0.0(0.0) ^c	180.0	180.0(180.0) ^c
O(4)–N(2)–O(3)–H(6)	—	0.0	0.0	180.0	134.2	—	0.0	0.0(0.0) ^c
H(7)–O(4)–N(2)–O(3)	—	—	—	—	—	—	180.0	—

^a Structure optimized at MP2/6-31G** level of theory. ^b Experimental values taken from ref. 8. ^c MP2/6-31G* calculated values taken from ref. 10.

Table 2 Total energies and zero point vibrational energies of **1**, **4a–c**, **MC1**, **MC1'**, N₂O, H₂O, HO[−], **7**, **8**, **9**, **10**, **10TS**, **11**, **11TS**, as well as decomposition products (N₂O + 2 (3) H₂O) calculated at MP2/6-31G + G** level of theory

Molecule	Energy/hartree ^a	ZPE ^b /kcal mol ^{−1}	E + ZPE/kcal mol ^{−1}
1	−260.37959	24.4	−163366.3
4a	−260.36126	23.1	−163356.1
4b	−260.36230	23.5	−163356.3
4c	−260.36254	23.6	−163356.4
MC1	−259.83181	12.6	−163034.3
MC1'	−259.83082	12.5	−163033.8
N ₂ O	−184.21442	6.3	−115590.0
HO [−]	−75.60211	5.3	−47435.7
H ₂ O	−76.23311	13.1	−47823.9
7	−259.82619	16.1	−163027.3
8	−260.64680	30.6	−163527.7
9	−260.67294	31.1	−163543.6
10	−336.60549	37.7	−211185.4
10TS	−336.59140	35.1(935.8i cm ^{−1}) ^c	−211179.2
N ₂ O + 2 H ₂ O	−336.69874	36.0	−211245.7
11	−412.85439	53.3	−259016.8
11TS	−412.84382	50.4(830.6i cm ^{−1}) ^c	−259013.0
N ₂ O + 3 H ₂ O	−412.94826	51.6	−259077.4

^a One hartree = 4.359 7482(26) × 10^{−18} J. ^b The zero point energy is scaled by 0.9646. ^c The value of the negative frequency.

minima located on the potential energy surface for the decomposition of complexes investigated was confirmed by IRC calculations as implemented in the Gaussian 94 package.²¹ Atomic charges were derived by Löwdin partitioning of the electron density distribution based on the symmetrically orthogonalised atomic orbitals.¹⁷

Computational results and discussion

Calculated bond distances and angles of nitramide (**1**) and its *aci*-nitro tautomers (**4a–d**) are shown in Table 1, while energy-related information is listed in Table 2. Also included are the structural parameters and energies of other isolated molecules, ions, and complexes investigated in this work shown in Fig. 1 and 2 (see below), as well as N₂O, HO[−], and H₂O. Although some of these ions and molecules, including **1** and **7**, were the subjects of previous experimental^{8,10,13,22} and computational^{9,10} studies, calculations on them have been repeated to provide a

reference for our results on other species studied in the present work. It is satisfying to note that the calculated structure of **1**, in particular, is in good agreement with earlier computational results⁹ and with the best experimental determinations.^{8,22}

Isomerisation of **1** to the *aci*-nitro form, which is postulated to be a crucial step in nitramide hydrolysis,¹³ could result in *E* or *Z* diastereoisomers, each of which has conformational isomers. In the present work, we were able to locate only **4a–c** as true local minima at all levels of theory employed. Structure **4d** appeared to be a minimum only at the MP2/6-31G** level (Table 1), while all other methods predicted it to have one negative vibrational frequency (231.6i cm^{−1} at MP2/6-31G+G** and 318.9i cm^{−1} at MP2/6-311+G**) corresponding to rotation of the hydroxy group around the N(2)–O(3) bond.

Scrutiny of the calculated structural parameters in Table 1 shows that all *aci*-nitro forms (except **4d**) are completely planar with each hydroxy hydrogen atom held in the plane by an

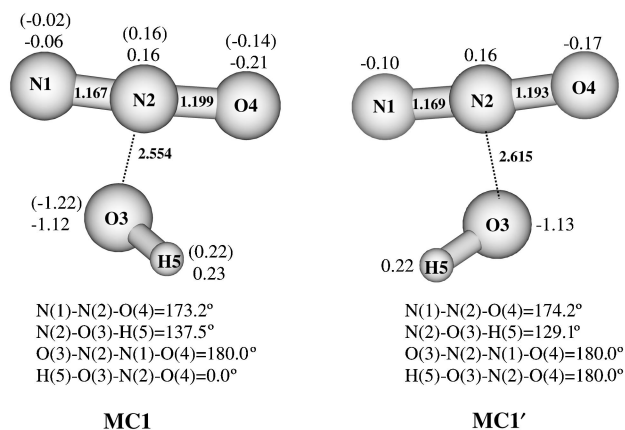


Fig. 2 The optimised geometries of the loosely bonded bimolecular complexes **MCI** and **MCI'**. Distances are given in Ångstroms and angles in degrees. The distribution of the atomic charge in **MCI** and **MCI'**, and in the fully separated N_2O and HO^- (in parentheses) is also given.

intramolecular hydrogen bond. Another common feature is that all structures exhibit some degree of delocalisation, but each principal contributing resonance structure appears to be the one with an N(1)–N(2) double bond. An important result from Table 2 is that isomers **4a–c** are of comparable stability (within 0.5 kcal mol⁻¹) with only a slight energetic preference for **4c** which, interestingly, is the isomer predicted to have the largest degree of delocalisation. Nevertheless, because of their similar energies, all three isomers are expected to be present in equilibrium in liquid media, although this will also be affected by entropy considerations which have not been calculated.

Each of the *aci*-nitro isomers possesses alternative deprotonation sites, the hydroxylic oxygen O(3) and the imino nitrogen N(1). Deprotonation from N(1) to give anion **5** is more pertinent to the present discussion. All attempts to locate this anion starting from the optimised geometry of any of the *aci*-nitro structures, however, failed. In each case, the structure obtained by removal of the imidic hydrogen dissociated spontaneously during optimisation to a loosely bound bimolecular complex of nitrous oxide and hydroxide, but we were unable to locate a transition structure for this decomposition. It is worth noting that the relative orientation of the N_2O and HO^- fragments in the resulting complex depends on the configuration and conformation of the starting *aci*-nitro molecule. Thus, deprotonation of either **4a** or **4b** leads to the structure represented by **MCI** in Fig. 2, while optimisation of the deprotonated structure **4c** results in the **MCI'** complex. Both structures were characterised as local minima on the PES, the former being slightly (0.5 kcal mol⁻¹) more stable than the latter (Table 2). Similarly, their geometrical parameters are almost identical with the exception of the N(2)–O(3) distance, which is found to be 0.061 Å longer in **MCI'** than in **MCI** (Fig. 2).

Significantly, the hydration energy of complex **MCI'** calculated by the IPCM method was found to be greater than that of **MCI** (Table 3), leading to a reversal in their relative stabilities compared with in the gas phase.

Interestingly, the linear hydrogen-bonded structure $\text{NN}^+-\text{O}^- \cdots \text{HO}^-$ could not be located on the PES, indicating that the interaction between the negative oxygen of HO^- and the positive middle nitrogen of N_2O is stronger than the hydrogen bond between the hydroxide proton and the negative oxygen of the N_2O molecule.

At the MP2/6-31G+G** level, complexes **MCI** and **MCI'** lie 8.6 kcal mol⁻¹ and 8.1 kcal mol⁻¹, respectively, below the energy of the fully separated products, N_2O and HO^- . Inclusion of the correction for the BSSE calculated using the counterpoise method²³ reduces the intermolecular interaction energy by ca. 2.0 kcal mol⁻¹ at the MP2/6-31G+G** level of theory for

Table 3 Total energies and energies of solvation (ΔE_{sol}^b) of **MCI**, **MCI'**, **10**, **10TS**, **11**, **11TS**, N_2O , OH^- , as well as of decomposition products ($\text{N}_2\text{O} + 2(3) \text{H}_2\text{O}$), in water calculated at the MP2/6-31G+G**//MP2/6-31G+G** level of theory

Molecule	Energy (water)/hartree ^a	$\Delta E_{\text{sol}}^b/\text{kcal mol}^{-1}$
MCI	-259.94197	69.1
MCI'	-259.94634	72.5
10	-336.62044	9.4
10TS	-336.60249	7.0
$\text{N}_2\text{O} + 2 \text{H}_2\text{O}$	-336.71364	9.3
11	-412.87357	12.0
11TS	-412.86218	11.5
$\text{N}_2\text{O} + 3 \text{H}_2\text{O}$	-412.96510	10.6

^a One hartree = 4.359 7482(26) × 10⁻¹⁸ J. ^b $\Delta E_{\text{sol}} = E_{\text{water}} - E_{\text{gas phase}}$.

both complexes. We also compared the charge distribution in calculated complexes with that in their separated components using Löwdin partitioning of the electron density distribution (Fig. 2). It appears that the distribution of atomic charges in the N_2O and HO^- fragments in both complexes is slightly different from when they are fully separated. For example, effective charges are -1.22 and 0.22 in the isolated hydroxide ion compared with -1.12 and 0.23 in **MCI**, indicating that electron transfer from N_2O to the hydroxide in **MCI** is not complete. A corresponding slight surplus of negative charge (0.11 e) is calculated within the N_2O part of the complex. The same holds for complex **MCI'** (Fig. 2).

Finally, we have optimised the structural isomer of the non-existent **5**, *i.e.* anion **7**, obtained by deprotonation of the O(3) hydroxy of **4a–c**. Our calculated structure (Table 1) is in good agreement with the previously reported MP2(full)/6-31G* geometry.¹⁰

Protonated forms

Protonation of the *aci*-nitro isomers **4a–c** can occur at three different positions N(1), O(3), and O(4). The most relevant mode of protonation in relation to the acid-catalysed decomposition of nitramide is that occurring at O(3).¹³ Depending on the starting geometry of the *aci*-nitro form, this protonation mode could result in the formation of two isomeric conjugate acids, **6a** and **6b** (Fig. 1). Such species, if formed, are expected to be highly unstable (at least in the gas phase) due to unfavourable electrostatic interactions between adjacent positive charges at the N(2) and O(3) atoms; our calculations indicate that this is indeed the case. During the geometry optimisation, the N(2)–O(3) bond in both ions underwent a continuous elongation resulting in the separation of H_2O . Similar calculations were subsequently carried out for bimolecular complexes of a water molecule with **6a** and **6b** with the water molecule located 1.8 Å from the imidic hydrogen atom to allow proton abstraction from N(1). In both cases, the initial complex collapsed into H_3O^+ , N_2O and H_2O . Thus, ions **6a** and **6b** are not stable bonded species and cannot, therefore, be proper intermediates in the acid catalysed decomposition of nitramide by the mechanism in Scheme 5. Correspondingly, the step-wise mechanism of Scheme 7 for the acid-catalysed decomposition of alkyl-nitramides becomes questionable. The spontaneous cleavage induced by proton transfer in the present context is analogous to the concerted dissociation which may accompany electron transfer to some alkyl and aryl halides, an issue discussed recently by Savéant.²⁴

Regarding protonation at the other two positions, O(4) and N(1) of **4** leading to **8** (from **4a**) and **9** (from **4a** and **4b**) (Fig. 1), our MP2/6-31G+G** calculations predict N(1) (PA = 187.6 kcal mol⁻¹) to be more basic by ca. 16 kcal mol⁻¹, depending on the starting *aci*-nitro tautomer, than O(4) (PA = 171.7 kcal mol⁻¹). The N(1) protonated form of an *aci*-nitro tautomer corresponds, of course, to the thermodynamically favoured

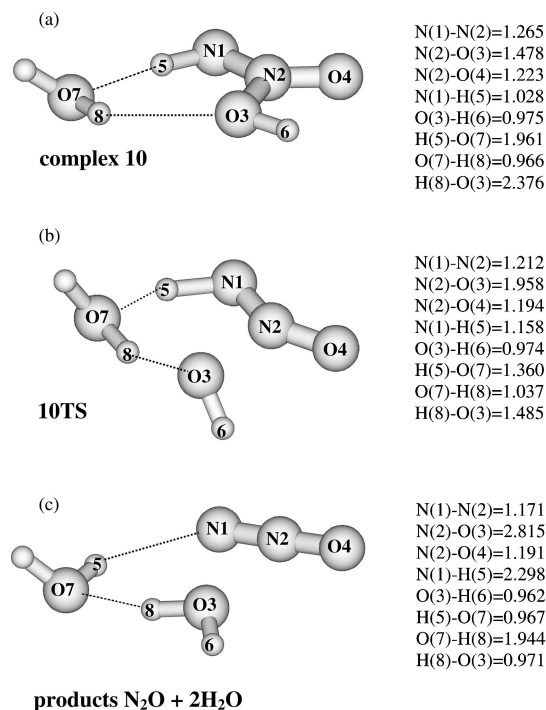


Fig. 3 (a) MP2/6-31G+G** optimised geometries of complex **10**, (b) transition structure **10TS**, (c) the corresponding decomposition products ($\text{N}_2\text{O} + 2\text{H}_2\text{O}$), distances in Ångstroms.

protonated form of **1** in the gas phase. Our calculated structure for **9** (Table 1) is in good agreement with the previously reported geometry for this species.¹⁰

Complexation of **4a** with water

In order to check Cox's proposal regarding the water-assisted decomposition of nitramide,¹³ complexation of **4a** with one and two water molecules in the gas phase, and in water, was explored. The MP2/6-31G+G** optimised structures of the cyclic complexes, **10** and **11**, are shown in Fig. 3a and 4a, respectively.²⁵ Interestingly, both complexes are found to be true minima on the corresponding PES within the framework of the theoretical model employed.²⁶ Complex **10** is found to be about 5.4 kcal mol⁻¹ more stable than the isolated reactants (**4a** + H_2O), while the stabilisation energy for the cyclic structure comprising **4a** and two water molecules, **11**, amounts to 12.9 kcal mol⁻¹. Inclusion of the correction for BSSE leads to stabilisation energies of 3.3 kcal mol⁻¹ and 7.9 kcal mol⁻¹ for **10** and **11**, respectively. Thus, energetically, **11** is favoured, but when entropy aspects are included (especially translational) the route *via* **10** could be the path of lower free energy. The most prominent structural feature of the optimised geometry of **11** is the presence of three hydrogen bonds which are all considerably shorter (about 1.9 Å) than typical intermolecular hydrogen bonds (2.4–2.9 Å).²⁶ In contrast, the hydrogen bond between O(3) and H(8) in complex **10** (2.376 Å) (Fig. 3a) is much closer to the typical values although the one from the imidic N–H to the water, O(7)–H(5), is short (1.961 Å).²⁶ Another interesting feature of the equilibrium geometry predicted for **10** and **11** concerns elongation of the N(2)–O(3) bond (by 0.031 Å and 0.065 Å in **10** and **11**, respectively) relative to its value in **4a** (1.447 Å).

We also tried to locate transition structures connecting **10** and **11** with their decomposition products, $\text{N}_2\text{O} + 2(3)\text{H}_2\text{O}$. Starting from the optimised structure of **10** led to structure **10TS** (Fig. 3b) which was shown to be a saddle point by vibrational analysis ($\nu = 835.8\text{ i cm}^{-1}$). Similarly, starting from the equilibrium geometry of **11**, we ended up with the transition structure **11TS** ($\nu = 830.6\text{ i cm}^{-1}$) (Fig. 4b). The connections of

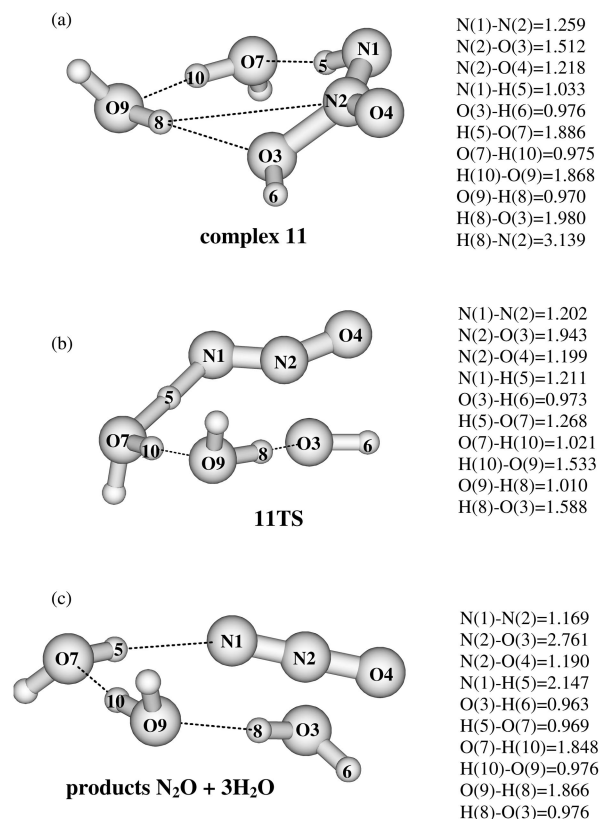


Fig. 4 (a) MP2/6-31G+G** optimised geometries of complex **11**, (b) transition structure **11TS**, (c) the corresponding decomposition products ($\text{N}_2\text{O} + 3\text{H}_2\text{O}$), distances in Ångstroms.

the proposed transition structures to their decomposition products (Fig. 3c and 4c) in the forward reaction, and to the starting complexes **10** and **11**, respectively, in the reverse reaction were confirmed by subsequent IRC calculations. We note that **10TS** lies 6.2 kcal mol⁻¹ higher in energy than **10**, while **11TS** is only 3.8 kcal mol⁻¹ less stable than **11**. Comparison of the structures calculated for **11** and **11TS** (Fig. 4a and 4b) reveals that, on passing from **11** to **11TS**, the N(2)–O(3) bond lengthens from 1.512 to 1.943 Å. This is accompanied by an increase in the N(1)–H(5) bond length of 0.178 Å and a more pronounced decrease of 0.618 Å in the O(7)–H(5) distance, H(5) being the migrating proton. Also, structure **11TS** includes quite close contact between the hydroxy group and the nearest water molecule (1.588 Å) as well as a short hydrogen bond (1.533 Å) between the two water molecules. Similar trends, although somewhat less pronounced, are observed on passing from **10** to **10TS**. Thus, the migrating proton H(5) is less transferred in **10TS** (N(1)–H(5) = 1.158 Å) than in **11TS** (N(1)–H(5) = 1.211 Å). However, the N(2)–O(3) bond in **11TS** is found to be even more tenuous than in **10TS**. Finally, we examined the effect of hydration on the relative stabilities of complexes **10** and **11** shown in Fig. 3 and 4, respectively, as well as their decomposition products and the corresponding transition structures. Our results show that hydration stabilizes all species considered, but to different extents. Specifically, for **10**, **10TS**, and their decomposition products, hydration energies are found to be 9.4, 7.0, and 9.3 kcal mol⁻¹, respectively (Table 3). The corresponding values for decomposition of **11** are 12.0, 11.5, and 10.6 kcal mol⁻¹, respectively (Table 3). As a consequence, the barrier height in both pathways increases in going from the gas phase into water, but the effect is more pronounced (and the process less favourable) in the mechanism involving one water molecule. All these calculated results are in accordance with the proposed water-assisted decomposition mechanisms of the *aci*-nitro form into N_2O and 2(3) H_2O ¹³ (Fig. 3 and 4). They also indicate that complexation with two water molecules in the

gas phase, as well as in water, is energetically more favourable, and that the potential energy barrier for the decomposition of the complex comprising two water molecules is lower than for a complex with just one water molecule. The results also allow us to refine Cox's mechanism involving two water molecules; the calculations indicate that cleavage of the N–OH bond runs ahead of the proton reorganisation, *i.e.* although the overall mechanism is concerted (no intermediates), the bond reorganisations are asynchronous. Again, however, entropy considerations could well favour the one-water molecule mechanism which would re-introduce uncertainty regarding the mechanism of lowest free energy.

Mechanisms

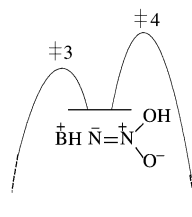
Acid–base aspects

Deprotonation of **1** gives anion **7** which may be reprotonated on either of two oxygens or the nitrogen. Reprotonation on oxygen gives **4a–c** any of which in principle could be intermediates in the decompositions of nitramide catalysed by acids or bases; Cox's mechanism for the water-induced reaction (Scheme 6) however, requires **4a**. Analogies indicate that the hydroxy protons of **4a–c** will be more acidic than the proton on nitrogen, but their loss only leads back to **7** whereas deprotonation from nitrogen leads to spontaneous decomposition (see below). When acting as a base, **4** has three sites for protonation in principle. However, only **8** and **9** (Fig. 1) are stable ions, and protonation of the hydroxy to give **6a** or **6b** leads directly to fragmentation, *i.e.* a concerted mechanism for the acid-catalysed decomposition (see below).

Base-catalysed decomposition of nitramide under mildly basic conditions

If k_4 is the rate-limiting step in the mechanism shown in Scheme 3 for the base-catalysed decomposition of nitramide, the anion **5** must have a finite lifetime. In the present study, however, we find that structure **5** does not correspond to an energy minimum; all attempts to minimise the energy of this structure led to dissociation to hydroxide and nitrous oxide. This theoretical result, however, corresponds to reaction in the gas phase, and ignores the effects of solvent and the counter-ion BH^+ in solution (although we have shown that **4a** is stabilised by two solvating water molecules), and entropy effects. Hydroxide and anion **5** are of the same charge type and both will be strongly solvated by hydrogen bonding in aqueous solution; the smaller and more polarising hydroxide will be the more strongly solvated and hence more stabilised in aqueous solution. Consequently, it is not easy to see how transfer of the reaction from the gas phase into aqueous solution will introduce a barrier between **5** and $\text{HO}^- + \text{N}_2\text{O}$, nor does consideration of entropy appear to favour the step-wise alternative. The closely associated cation BH^+ , however, provides a reaction for **5** which was not anticipated in our calculations on the isolated anion, *i.e.* proton transfer by the reverse of eqn. (3) (Scheme 3). This possibility allows reconciliation of the experimental work in solution and the computational results for the gas phase. The theoretical evidence indicates that the proton abstraction of eqn. (3) and the departure of the hydroxide in eqn. (4) are concerted and not separate steps. This does not require, however, that the concerted events be synchronous, and a

highly asynchronous single-step process would appear to accommodate the experimental results reported by Kresge and co-workers.¹¹ Scheme 8 represents the forward and back reactions of the putative intermediate **5**, step 4 and the reverse of step 3 in Scheme 3, with the former rate limiting as proposed earlier. The experimental results implicate **‡4** as the overall transition structure, *i.e.* with the proton *not* in flight, *but do not necessarily require* the preceding intermediate **5**; the theoretical results do not allow the existence of the anion **5** as an intermediate *but do not require fragmentation to hydroxide and nitrous oxide if an alternative is available*. Consequently, a single barrier late in the reaction coordinate for the concerted process corresponding to removal of the *first* barrier in Scheme 8



Scheme 8 Forward and reverse reactions of the putative intermediate **5** in Scheme 3.

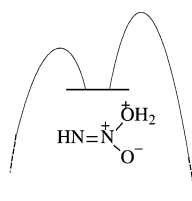
appears to accommodate all results. Thus, the rate-limiting step in the overall reaction, replacing steps 3 and 4 in Scheme 3, is a strongly asynchronous concerted process with the proton transfer virtually complete when the heavy atom reorganisation takes place in the transition state.

Base-catalysed decomposition of nitramide under strongly basic conditions

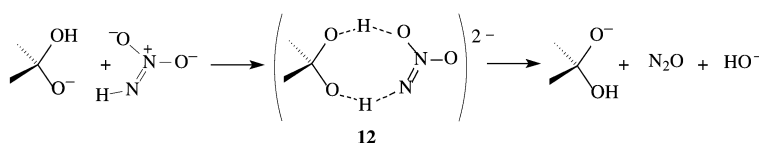
Kresge and co-workers established that bifunctional catalysts $\text{R}_2\text{C}(\text{OH})\text{O}^-$ are more effective than monofunctional ones RO^- and proposed a cyclic transition structure, **12** in Scheme 9.¹² This requires that the departing oxygen is the one *cis* to the hydrogen on nitrogen in the reaction involving bifunctional catalysis. Our attempts to investigate computationally whether *trans* elimination is more favourable than *cis* in an acyclic process were unsuccessful.

Acid-catalysed decomposition of nitramide and *N*-alkylnitramines

On the basis of the earlier experimental evidence,¹³ the acid-catalysed decomposition of **4** formed from **1** in Scheme 5 may proceed, in principle, *via* either diastereoisomer of $\text{HN}=\text{N}(\text{O})\text{OH}_2^+$, **6a** or **6b**; Scheme 10 is a profile representing part of Cox's mechanism, *i.e.* reversible protonation followed



Scheme 10 Forward and reverse reactions of the putative intermediate **6** in the acid catalysed-decomposition of nitramide, Scheme 5.



Scheme 9 Cyclic mechanism for bifunctional catalysis in the decomposition of nitramide.

by rate-limiting fragmentation of the intermediate. In attempting to establish which of **6a** or **6b** is the more stable, our calculations indicated that neither corresponds to a stable structure. This indicates that protonation of the hydroxys of both diastereoisomers of **4** and subsequent fragmentations are concerted (and hence the overall reaction should be general acid catalysed), but we were unable to identify the more favourable stereochemistry. Scheme 10, therefore, needs to be replaced by a single barrier profile but there is insufficient evidence yet to identify the position of the maximum within the reaction coordinate. It is improbable that *N*-alkylation will affect the viability of either **6a** or **6b** in which case the step-wise mechanism for the acid-catalysed decomposition shown in Scheme 7 needs to be replaced by an alternative in which the fragmentation is concerted with the preceding proton transfer. On the basis of evidence from the investigation of the acid-catalysed decomposition of *N*-alkyl-*N*-nitrosohydroxylamines,²⁷ this should lead to RN₂O⁺ as an intermediate which will undergo subsequent unimolecular or bimolecular hydrolytic conversion to ROH and nitrous oxide according to the nature of the R group.

Water-induced reaction

Cox's evidence appears to allow a mechanism for the uncatalysed reaction involving a single water molecule, structure **10**, rather than two as in transition structure **11** (Scheme 6).¹³ However, our calculations indicate that a process *via* structure **10** is less favourable than that shown in Scheme 6 with two molecules of water in strong support of Cox's proposal.

Acknowledgements

We thank the British Council and the Croatian Ministry of Science and Technology for a grant under the ALIS programme, and the Rudjer Boskovic Institute for computational facilities. We also gratefully acknowledge helpful comments on the manuscript by Professors R. A. Cox and A. J. Kresge.

References

- 1 J. N. Brønsted and K. J. Pedersen, *Z. Phys. Chem.*, 1924, **108**, 185; a good review of early work on the base-catalysed decomposition of nitramide is given by R. P. Bell, in *The Proton in Chemistry*, Chapman and Hall, 2nd edn., 1973. See also J. Hine, *Physical Organic Chemistry*, McGraw-Hill, 2nd edn., 1962; and L. P. Hammett, *Physical Organic Chemistry*, McGraw-Hill, 1st edn., 1940.
- 2 J. N. Brønsted, *Recl. Trav. Chim.*, 1923, **42**, 718; J. N. Brønsted and E. A. Guggenheim, *J. Am. Chem. Soc.*, 1927, **49**, 2554.
- 3 C. A. Marlies and V. K. La Mer, *J. Am. Chem. Soc.*, 1935, **57**, 1812; M. N. Hughes, J. R. Lusty and H. L. Wallis, *J. Chem. Soc., Dalton Trans.*, 1983, 261.
- 4 H. Maskill, P. Murray-Rust, J. T. Thompson and A. A. Wilson, *J. Chem. Soc., Chem. Commun.*, 1980, 788; H. Maskill, J. T. Thompson and A. A. Wilson, *J. Chem. Soc., Chem. Commun.*, 1981, 1239; H. Maskill and W. P. Jencks, *J. Chem. Soc., Chem. Commun.*, 1984, 944; H. Maskill, J. T. Thompson and A. A. Wilson, *J. Chem. Soc., Perkin Trans. 2*, 1984, 1693; H. Maskill and W. P. Jencks, *J. Am. Chem. Soc.*, 1987, **109**, 2062.
- 5 P. M. W. Gill, H. Maskill, D. Doppinger and L. Radom, *J. Chem. Res. (S)* 1987, 54. See also K. Yamashita and K. Morokuma, *Chem. Phys. Lett.*, 1986, **131**, 237.
- 6 W. P. Jencks, *Acc. Chem. Res.*, 1980, **13**, 161.
- 7 C. A. Beevers and A. F. Trotman-Dickinson, *Acta Crystallogr.*, 1957, **10**, 34.
- 8 J. K. Tyler, *J. Mol. Spectrosc.*, 1963, **11**, 39.
- 9 J. P. Ritchie, *J. Am. Chem. Soc.*, 1989, **111**, 2517; S. Roszak and J. J. Kaufman, *Chem. Phys.*, 1992, **160**, 1.
- 10 M. Attinà, F. Cacace, E. Ciliberto, G. de Petris, F. Grandinetti, F. Pepi and A. Ricci, *J. Am. Chem. Soc.*, 1993, **115**, 12398.
- 11 C. H. Arrowsmith, A. Awwal, B. A. Euser, A. J. Kresge, P. P. T. Lau, D. P. Onwood, Y. C. Tang and E. C. Young, *J. Am. Chem. Soc.*, 1991, **113**, 172.
- 12 C. H. Arrowsmith, A. J. Kresge and Y. C. Tang, *J. Am. Chem. Soc.*, 1991, **113**, 179.
- 13 R. A. Cox, *Can. J. Chem.*, 1996, **74**, 1779.
- 14 R. A. Cox, *Can. J. Chem.*, 1996, **74**, 1774.
- 15 H. Maskill, *J. Chem. Soc., Chem. Commun.*, 1986, 1433.
- 16 M. J. Frisch, G. W. Trucks, H. B. Schlegel, P. M. W. Gill, B. G. Johnson, M. A. Robb, J. R. Cheeseman, T. Keith, G. A. Petersson, J. A. Montgomery, K. Raghavachari, M. A. Al-Lanam, V. G. Zakrzewski, J. V. Ortiz, J. B. Foresman, J. Cioslowski, B. B. Stefanov, A. Nanayakkara, M. Challacombe, C. Y. Peng, P. Y. Ayala, W. Chen, M. W. Wong, J. L. Anders, E. S. Replogle, R. Gomperts, R. L. Martin, D. J. Fox, J. S. Binkley, D. J. Defrees, J. Baker, J. P. Stewart, M. Head-Gordon, C. Gonzalez and J. A. Pople, *GAUSSIAN 94, Revision C.2*, Gaussian, Inc., Pittsburgh PA, 1995.
- 17 M. W. Schmidt, K. K. Baldrige, J. A. Boatz, S. T. Elbert, M. S. Gordon, J. H. Jensen, S. Koseki, N. Matsunaga, K. A. Nguyen, S. J. Su, T. L. Windus, M. Dupuis and J. A. Montgomery, *J. Comput. Chem.*, 1993, **14**, 1347.
- 18 W. J. Hehre, L. Radom, P. v. R. Schleyer and J. A. Pople, *Ab Initio Molecular Orbital Theory*, Wiley, New York, 1986; G. Winkelhofer, R. Janoschek, F. Fratev, G. W. Spitznagel, J. Chandrasekhar and P. v. R. Schleyer, *J. Am. Chem. Soc.*, 1985, **107**, 332.
- 19 S. Scheiner, in *Reviews in Computational Chemistry*, ed. K. B. Lipkowitz and D. B. Boyd, VCH, New York, vol. 2, 1991, pp. 172–179.
- 20 K. B. Wiberg, P. R. Rablen, D. J. Rush and T. A. Keith, *J. Am. Chem. Soc.*, 1995, **117**, 4261; J. B. Foresman, T. A. Keith, K. B. Wiberg, J. Snoonian and J. M. Frisch, *J. Phys. Chem.*, 1996, **100**, 16098.
- 21 K. Fukui, *Acc. Chem. Res.*, 1981, **14**, 363; K. Ishida, K. Morohuma and A. Kormornichi, *J. Chem. Phys.*, 1977, **66**, 2153; M. W. Schmidt, M. S. Gordon and M. Dupuis, *J. Am. Chem. Soc.*, 1985, **107**, 2585.
- 22 N. I. Sadova, G. E. Slepnev, N. A. Tarasenko, A. A. Zeukin, L. V. Vilkov, I. F. Shiskov and Y. A. Paukrushev, *Zh. Strukt. Khim.*, 1977, **18**, 865.
- 23 S. F. Boys and F. Bernardi, *Mol. Phys.*, 1970, **19**, 553; F. B. van Duijneveldt, J. G. C. M. van Duijneveldt-van de Rijdt and J. H. van Lenthe, *Chem. Rev.*, 1994, **94**, 1873.
- 24 J.-M. Savéant, *Adv. Phys. Org. Chem.*, 2000, **35**, 117.
- 25 At the G2 level of theory, however, complex **10** corresponds to the transition structure ($\nu = 108.8i \text{ cm}^{-1}$).
- 26 S. Scheiner, *Hydrogen Bonding. A Theoretical Perspective*, Oxford University Press, New York, 1997.
- 27 H. Maskill, I. D. Menneer and D. I. Smith, *J. Chem. Soc., Chem. Commun.*, 1995, 1855; J. I. Bhat, W. Clegg, M. R. J. Elsegood, H. Maskill, I. D. Menneer and P. C. Miatt, *J. Chem. Soc., Perkin Trans. 2*, 2000, 1435.